Journal of Alloys and Compounds 509 (2011) 9906–9911

Contents lists available at ScienceDirect

Journal of Alloys and Compounds

journal homepage: www.elsevier.com/locate/jallcom

Thin films of thermoelectric compound Mg_2Sn deposited by co-sputtering assisted by multi-dipolar microwave plasma

H. Le-Quoc[a,b,*], A. Lacoste[a], E.K. Hlil[b], A. Bès[a], T. Tan Vinh[a], D. Fruchart[b], N. Skryabina[c]

[a] Laboratoire de Physique Subatomique et de Cosmologie - CNRS/UJF/Grenoble INP, 53 rue des Martyrs, 38026 Grenoble, Cedex, France
[b] Institut Néel, CNRS, BP 166, F-38042, Grenoble, Cedex 9, France
[c] Department of Physics, Perm State University, 614990 Perm, Russia

ARTICLE INFO

Article history:
Received 16 May 2011
Received in revised form 26 July 2011
Accepted 28 July 2011
Available online 3 August 2011

Keywords:
Mg_2Sn
Thin films
Thermoelectric
Plasma co-sputtering

ABSTRACT

Magnesium stannide (Mg_2Sn) thin films doped with Ag intended for thermoelectric applications are deposited on both silicon and glass substrates at room temperature by plasma assisted co-sputtering. Characterization by scanning electron microscopy, energy-dispersive X-ray spectroscopy and X-ray diffraction confirms the formation of fine-grained polycrystalline thin films with thickness of 1–3 μm. Stoichiometry, microstructure and crystal structure of thin films are found to vary with target biasing and the distance from targets to substrate. Measurements of electrical resistivity and Seebeck coefficient at room temperature show the maximum power factor of $\sim 5.0 \times 10^{-3}$ W K^{-2} m^{-1} for stoichiometric Mg_2Sn thin films doped with ~1 at.% Ag.

1. Introduction

Thermoelectric (TE) materials can convert thermal energy directly into electricity and vice versa through Seebeck and Peltier effect respectively, making them attractive for waste heat conversion and active cooling applications. Performances of TE materials refer to the figure of merit $ZT = (S^2\sigma/\lambda)T$, where S is the Seebeck coefficient, σ the electrical conductivity, λ the thermal conductivity, and T is the absolute temperature. Despite continuous progress, the best applied TE materials show ZT of no more than 1, so that the thermoelectric efficiency of those devices is only ~10% of Carnot efficiency [1]. Among promising TE materials, intermetallic compounds of Mg_2X type (X = Si, Ge, Sn) and related solid solutions were long time considered suitable for waste heat recovery and other energy conversion applications in the 500–800 K temperature range [2]. These narrow band gap semiconductor compounds exhibit many advantages for potential TE applications, notably the abundance of constituents, low density, as well as non-toxicity and environmental friendliness. Recently, bulk state solid solutions of Mg_2Si–Mg_2Sn with $ZT_{max} = 1.1$ at ~800 K were reported for *n*-type materials [3,4]. On the other hand, it has been showed that nanostructuring of TE materials could reduce the thermal conductivity by phonon scattering in nanosized crystals while enhance, or at least maintain, the electrical conductivity level, thereby increasing ZT [5]. Synthesis of Mg_2X in thin films thus could provide further control of the microstructure, and more interestingly their nanostructure, in order to enhance the thermoelectric performance. In addition to the fundamental benefit of nanostructuring in reducing the thermal conductivity, the rising interest for TE thin films relies in the miniaturizing ability and integration of TE modules into devices to attain a higher power density [6]. Recent works on Ag-doped Mg_2Ge thin films deposited by magnetron co-sputtering have showed that a single-phase polycrystalline Mg_2Ge thin films can be obtained at substrate temperatures ranging from 600 to 1000 K and exhibit power factors up to 6×10^{-4} W K^{-2} m^{-1} at ~600 K [7], noting that this value is still an order of magnitude lower than that of the current best commercial TE materials based on Bi_2Te_3.

The aim of the present work is to study and achieve the controlled deposition of Mg_2Sn based thin films by plasma assisted co-sputtering of individual targets of the constituent elements. For this purpose, an original plasma technology was used which enables a large flexibility of the sputtering process, thanks to the complete decoupling between the plasma production (supply power and gas) and the biasing of targets as well as that of substrate. Such a complete decoupling offers an independent control of both flux and energy of deposited particles. In fact this can allow us to control the stoichiometry, microstructure and crystal structure of the deposited thin films. Thin films with room temperature (RT) power factor comparable to that of bulk Bi_2Te_3 based TE materials

* Corresponding author at: Laboratoire de Physique Subatomique et de Cosmologie de Grenoble, Centre de Recherche Plasmas-Materiaux-Nanostructures, 53 rue des Martyrs, 38026 Grenoble Cedex, France. Tel.: +33 4 76 28 41 66.
E-mail addresses: huy.le-quoc@lpsc.in2p3.fr (H. Le-Quoc), ana.lacoste@ujf-grenoble.fr (A. Lacoste).

0925-8388/$ – see front matter © 2011 Elsevier B.V. All rights reserved.
doi:10.1016/j.jallcom.2011.07.085

Table 1
Composition and thickness of thin films deposited with different bias voltages of Ag-doped Sn targets and target–substrate distances.

Bias voltage of Ag-doped Sn targets (V)	Mg content (at.%)	Sn content (at.%)	Ag content (at.%)	Mg:Sn	Thickness (μm)
Distance target–substrate h = 120 mm					
−100	72.6	23.2	4.2	3.1	2.8
−200	59.2	37.2	3.6	1.6	1.9
−230	62.5	36.8	0.7	1.7	2.2
−250	60.9	37.9	1.2	1.6	2.3
−300	59.5	39.3	1.1	1.5	2.4
Distance target–substrate h = 200 mm					
−230	61.1	37.6	1.3	1.6	1.0
−250	59.8	39.2	1.0	1.5	1.3

were indeed obtained for samples with Mg:Sn = 2:1 stoichiometry and with the crystallite size of less than 100 nm.

2. Experimental

2.1. Deposition of thin-films by assisted multi-dipolar microwave plasma co-sputtering

Sputtering methods are widely used for thin film deposition, especially in microelectronic devices fabrication [8]. Compared to other deposition processes, such as thermal evaporation and chemical vapor deposition, a unique feature of the very low-pressure sputtering lies in the energy of deposited species. Indeed, at very low-pressure, thus in absence of elastic collisions between target and substrate, the energy distribution function of the deposited atoms corresponds to that of sputtered atoms, with a mean energy of the order of their vaporization energy. This relatively high-energy of deposited species, which can be concurrently assisted by ion bombardment at substrate, leads to the growth of thin films far from thermodynamic equilibrium.

The flexibility in terms of operating parameters is a critical requirement in the deposition processes in order to facilitate the control of the thin-films properties. Consistent with this required suppleness, the sputtering is performed in the multi-dipolar microwave plasma (MDMP) reactor developed at LPSC laboratory [9,10]. As shown in the scheme of Fig. 1, the auxiliary plasma is sustained by electron cyclotron resonance at the end of each individual elementary microwave applicators distributed over the periphery of the chamber. Targets and substrate, both immersed in the plasma chamber, can be simultaneously and independently biased. By an appropriate adjustment of operating parameters (microwave power, working gas pressure, target and substrate biasing, target–substrate distance and substrate temperature) an accurate and independent control of both the flux and energy of deposited particles can be achieved. The MDMP technology hence permits synthesize thin-films of complex alloys with well-defined stoichiometry and optimized micro-structure. In addition this technique allows scaling up to large surface, uniform target erosion, and continuous sequential processes (cleaning, deposition). All these features make this plasma sputtering deposition technology distinct from the other ones, such as DC or RF magnetron sputtering.

Thin films of binary intermetallic compounds Mg_2Sn with Ag doping (for p-type) are grown on both Si (1 0 0) and Si (1 1 1) substrates (15 × 15 × 0.35 mm) as well as glass substrates (fused silica) (10 × 25 × 1 mm) by co-sputtering Mg and Sn from targets of ⌀ 60 × 10 mm thick. To introduce doping elements, Sn targets are prior doped with 2 at.% Ag. The base pressure in the plasma chamber is maintained less than 4×10^{-5} Pa and the working pressure of the argon gas is fixed at 1.5 mTorr (0.2 Pa). For 2 kW of microwave power, the plasma density was as high as 7.45×10^{11} cm^{-3}, yielding a sputtered current density of about 3 mA/cm^2 on targets.

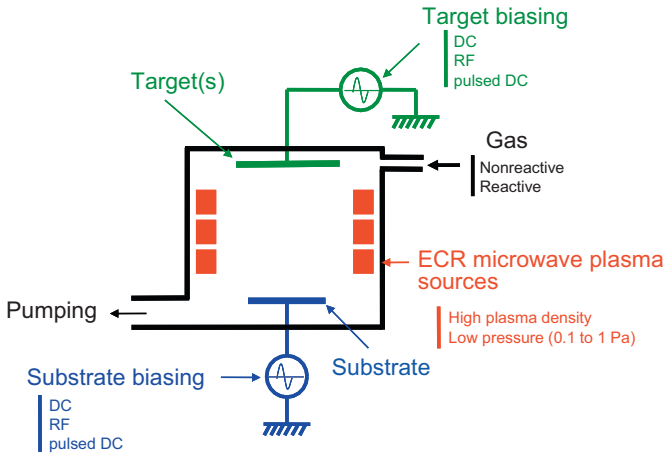

Fig. 1. Schematic diagram of the microwave plasma sputtering equipment used for thin film deposition.

Prior to each film growth, *in situ* cleaning of the substrate is carried out for 10 min in argon plasma by applying a bias voltage of −20 V to the substrate. Also to eliminate the impurity layer formed on the targets surface during prior depositions all targets are cleaned by applying a bias voltage of −200 V during 10 min. All samples are grown on substrates in thermal contact with the substrate-holder maintained at RT by water cooling. Due to the concurrent argon ion bombardment and the condensation energy of deposited particles, the effective temperature at the substrate surface may be higher than RT.

The composition, *i.e.* Mg and Sn contents, of the thin films is controlled by independently adjusting the bias voltage of Mg and Sn targets. For a desired composition, the bias voltage of targets is firstly estimated from the sputtering yield of each target material by using the formula proposed in Ref. [11]. The possibility to control the microstructure of thin films is studied by adjusting the distance between targets and substrate, since this distance can affect the deposition rate and energy of deposited particles. Distances from targets to substrate of 120 and 200 mm are considered here. We start by working at the target–substrate distance of 120 mm, with the bias voltage of Ag-doped Sn targets varied from −100 to −350 V while that of Mg targets is fixed at −450 V. The bias voltage of the Ag-doped Sn targets is intentionally chosen in this range in order to obtain thin films with varied composition, *i.e.*, from Mg-rich to stoichiometric Mg_2Sn, and to Sn-rich sides. For the target–substrate distance of 200 mm, films are deposited only with the bias voltages of Ag-doped Sn targets that were found corresponding to the stoichiometric Mg_2Sn films during depositions at the target–substrate distance of 120 mm. It should be noted that in our operating conditions, *i.e.*, a plasma potential of about 20 V and the substrate connected to ground, growing films are subjected to an ion bombardment with ions energy ~20 eV. The thickness of deposited thin films is directly adjusted by the deposition time, which is chosen of 2 h in this work.

2.2. Characterization of thin films

Composition of the obtained thin films is measured by Energy Dispersive X-ray spectroscopy (EDS) using a field-emission scanning electron microscopy (FESEM) ZEISS ULTRA Plus equipped with a Brukers Quantax 200 detector. Final composition is deduced by averaging the values of at least 10 points on the entire film surface. The incident electron accelerating voltage is 15 kV and quantitative analyses are carried out with $\Phi(\rho z)$ correction using standards of MgO, pure Sn, and pure Ag. Both surface and cross-section microstructure of deposited thin films are investigated by FESEM (ZEISS ULTRA Plus). Film thickness is estimated from SEM images of fracture cross-section. Crystal phase analysis and preliminary investigation of preferential film growth direction (texture) are performed by X-ray diffraction (XRD) in reflection mode using the standard θ–2θ Bragg-Brentano geometry at $\lambda_{Cu-K\alpha1}$ with a Bruker D8 Advance diffractometer. The whole profile fitting is then carried out, when applicable, to refine the lattice parameter and peaks broadening, using FullProf program [12]. During these refinements, the pseudo-Voigt profile function is used to model the peak broadening [13]. Crystallite size is roughly estimated by using the Scherrer formula [14] after correcting the instrumental broadening measured with the standard material LaB_6 (NIST SRM 660a). Texture of samples exhibiting strong preferential orientation is further verified by using an X-ray pole figure diffractometer (SEIFERT Debyeflex 3003).

Preliminary estimates of TE performance of deposited thin films (electrical resistivity and Seebeck coefficient) are carried out at RT. Room temperature electrical resistivity (ρ) is measured by the standard 4-points probe method using an automated measuring system (Lucas Signatone Pro4-4000). The Seebeck coefficient (S) is determined by applying a small temperature gradient $\pm\Delta T$ on the sample via two heaters and recording the TE voltage ΔV. A linear regression is then applied to the ΔV–ΔT data to define the slope thus deduce S. Hall effect measurements at room-temperature are carried out on 5 × 5 mm specimens cut from deposited samples, using bar Hall configuration with 4 silver contacts deposited on films surface by RF magnetron sputtering. During these measurements, the current is fixed at 1 mA and the magnetic field varies from −5 to 5 T.

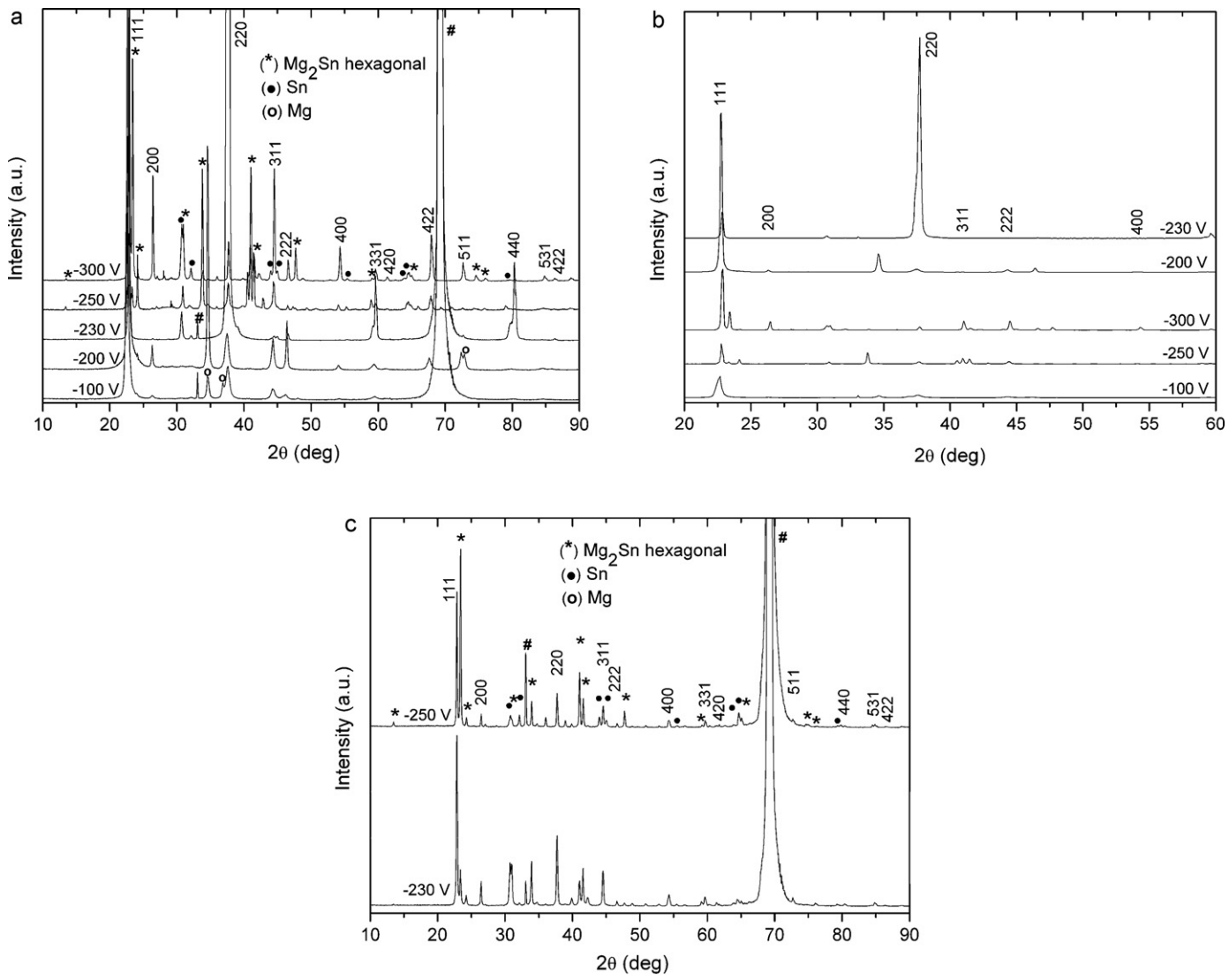

Fig. 2. X-ray diffraction patterns of Mg_2Sn thin films deposited on Si (1 0 0) substrates, for different bias voltages of Ag-doped tin targets (Mg targets biasing fixed at −450 V), and with the target–substrate distance of 120 mm (a, b), and 200 mm (c). Sharp and intense peaks (#) are due to Si substrates. Note that because of strong texture of thin films to (1 1 1) or (2 2 0) plans (see text and (b)), in (a) diffraction patterns are zoomed out in order to see all the peaks of Mg_2Sn cubic phase.

3. Experimental results

3.1. Composition, crystal structure and morphology of thin films

EDS analyses show homogenous composition on the entire surface of all obtained thin films. As expected, film composition varies with the bias voltage of Ag-doped Sn targets and is nearly unchanged when the distance target-to-substrate changes from 120 to 200 mm (Table 1). Within the error of the quantitative EDS analysis, we can see that stoichiometric Mg_2Sn thin films should be obtained with the Ag-doped Sn targets bias voltage in the range of −200 to −250 V, consistent with composition deduced from calculated sputtering yield. This result is further confirmed by XRD analysis (Fig. 2) and hence shows that thin films with composition varying from Mg-rich side, to stoichiometric Mg_2Sn, and up to Sn-rich side are obtained. The presence of Ag doping element was confirmed for all thin films. The Ag content is around 1 at.%, *i.e.* near the nominal value (about 0.7 at.%), for thin films of stoichiometric Mg_2Sn, but somewhat higher for films deposited at low bias voltages of Ag-doped Sn targets. From this result, two samples were deposited with pure Sn targets biased at −230 V and −250 V in order to obtain undoped Mg_2Sn thin films.

Fig. 2a shows XRD patterns of thin films deposited with different bias voltages of Ag-doped Sn targets, at the target–substrate distance of 120 mm. We note that at same bias voltages films deposited with pure Sn targets show almost identical XRD pattern to that of films deposited with Ag-doped Sn targets. It can be seen that all samples exhibit the C15 Mg_2Sn cubic structure corresponding to ICSD card 007-0274 (space group Fm3m, $a = 6.759$ Å). All films show more or less texture effect which is most pronounced for films deposited at the Ag-doped Sn targets biased at −200 and −230 V, with the fiber texture along the close-packed (1 1 1) and (2 2 0) planes, respectively (Fig. 2b). It is clearly seen that both phase composition and texture of thin films vary with the bias voltage of Ag-doped Sn targets. Indeed, with bias voltage of Ag-doped Sn targets below −250 V, deposited films are mostly composed of Mg_2Sn crystallized in the cubic phase, whereas for bias voltages of −250 V, the Mg_2Sn C14 hexagonal phase type Mg_2Zn corresponding to ICSD card 033-0866 (space group P63/m, $a = 13.180$ Å, $c = 6.990$ Å) begins to appear. The amount of hexagonal Mg_2Sn phase appears to increase at the highest applied bias voltage (*i.e.* −300 V), however the cubic C15 phase remains dominant. For low bias voltages of Ag-doped Sn targets, *i.e.* at −100 V and −200 V, the XRD patterns reveal residual peaks of pure Mg, while some peaks of β–Sn are observed at higher bias voltages (−230 to −300 V). This observation is consistent with the increase of the sputtering yield of Ag-doped Sn targets with bias voltage, while Mg targets are always biased at −450 V. Thin film with small residual peaks of Sn and without any peaks of Mg is obtained with Ag-doped Sn targets biased at −250 V. These results are in agreement with the compositions of thin films analysed by EDS. It is worth to emphasize that no specific difference in crystal structure is noticed between films deposited either on Si (1 0 0), Si (1 1 1), or fused silica substrates. For the target–substrate distance of 200 mm, films show less degree of texture when deposited with same bias voltages of Ag-doped Sn targets, here at −230 V and −250 V, *i.e.* corresponding to stoichiometric Mg_2Sn films (Fig. 2c). We can also notice that for these films the hexagonal phase of Mg_2Sn is more prominent com-

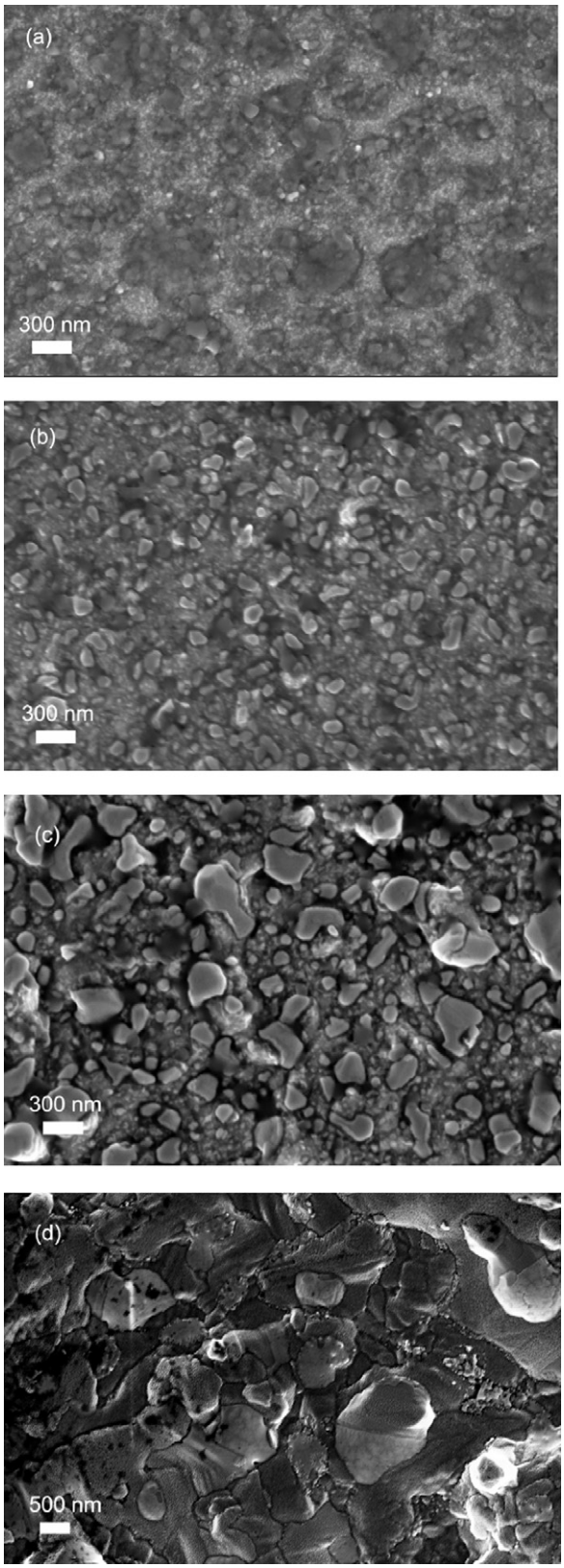

Fig. 3. Surface morphology of Mg_2Sn thin films deposited on Si (1 0 0) substrates, for different bias voltages of Ag-doped Sn targets: (a) −100 V, (b) −250 V and (c) −300 V, at 120 mm between targets and substrate; and (d) −250 V at 200 mm.

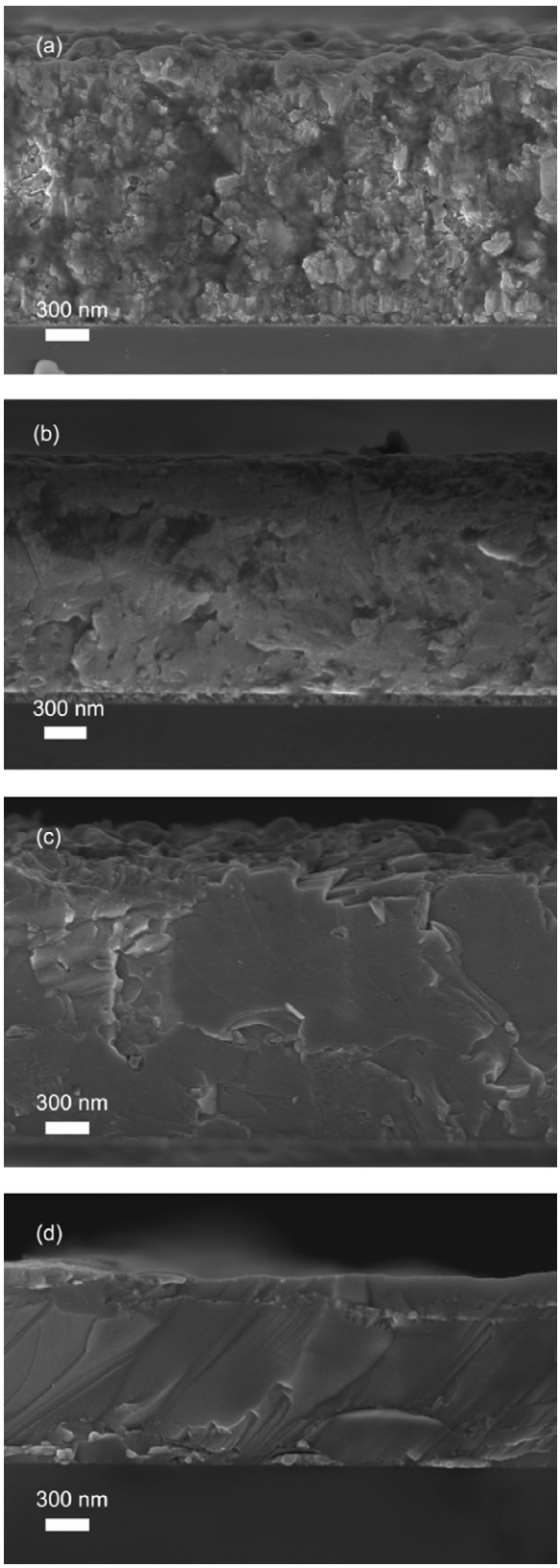

Fig. 4. Fracture cross-section morphology of thin films deposited on Si (1 0 0) substrates, for different bias voltages of Ag-doped Sn targets: (a) −100 V, (b) −250 V and (c) −300 V, at 120 mm between targets and substrate; and (d) −250 V at 200 mm.

Table 2
Electrical conductivity (σ), Seebeck coefficient (S) and thermoelectric power factor (σS^2) of Mg_2Sn thin films deposited on Si (1 0 0) substrates, for different bias voltages of Ag-doped Sn targets and target–substrate distances. Values in parentheses are for undoped films deposited with pure Sn targets at same deposition conditions.

Bias voltage of Ag-doped Sn targets (V)	σ (Ω^{-1} cm^{-1})	S (μV K^{-1})	$\sigma S^2 \times 10^{-3}$ (W K^{-2} m^{-1})
Distance target–substrate h = 120 mm			
−100	10695.4	21.2	0.48
−200	7972.5	68.6	3.75
−230	390.7 (25.2)	158.1 (−5.1)	0.98
−250	1051.6 (73.3)	203.5 (−100.2)	4.35
−300	1309.2	160.6	3.38
Distance target–substrate h = 200 mm			
−230	2847.7	120.3	4.12
−250	2059.9	156.1	5.02

pared with that of films deposited at the target–substrate distance of 120 mm.The formation of high-pressure and high-temperature phases, in the present case the C14 hexagonal phase of Mg_2Sn, as well as the high degree of films texture is usually observed in thin films deposited by sputtering. These effects could be explained by the formation of thin films in the condition far from thermodynamic equilibrium, and in particular with the high energy of sputtered atoms arriving at the substrate associated with ion bombardment on growing films [15]. The growth of Mg_2Sn polycrystalline thin films even at RT could be an evidence for highly energetic sputtered atoms. Furthermore, the formation of the hexagonal phase of Mg_2Sn should result here from the impact of the 2D-deposition on the initial cubic (1 1 1) texture. The C14 variant of Mg_2Sn was already reported to exist in bulk samples [16,17], as well as to appear when heating C15-type materials above ∼900 K [18]. It should be interesting to further investigate the formation of the Mg_2Sn hexagonal phase and its potential impact on the TE properties of thin films, noting that the C14 phase exhibits likely a more metallic behavior compared to the C15 one.

Surface morphology observed under FESEM of thin films is shown in Fig. 3. All thin films exhibit granular surfaces. For a given target–substrate distance, the lateral grain size increases with increasing bias voltage of Ag-doped Sn targets. Thin films deposited at the target–substrate distance of 120 mm have lateral grain size ranging from less than 100 to ∼400 nm as the bias voltage of Ag-doped Sn targets raises from −100 to −300 V (Fig. 3a–c). For the same bias voltage, the lateral grain size increases as the target–substrate distance increases from 120 mm to 200 mm (Fig. 3b and d). Broad peaks of the XRD patterns suggest thin films with finer crystallites and thus we roughly estimate the mean crystallite size by applying the Scherrer formula. For films deposited at the target–substrate distance of 120 mm, mean crystallites size ranges from ∼15 to ∼55 nm when the bias voltage of Ag-doped Sn targets increases from −100 to −300 V. Mean crystallite size is higher for films deposited at the longer target–substrate distance (*i.e.* at 200 mm), being ∼190 nm for bias voltage of Ag-doped Sn targets at −230 V and −250 V. The crystallite size is considerably smaller than that of grain size, suggesting that each grain is composed of many crystallites and this could be beneficial because grain boundaries between crystallites can effectively scatter the phonon propagation, thus reduce the thermal conductivity of thin films.

Fig. 4 shows typical fracture cross-section views of Mg_2Sn thin films. All thin films exhibit the typical morphology of zone T in the Structure Zone Diagram (SZD) [19], which is usually observed in sputter deposited thin films. It can be seen that at low bias voltage of Ag-doped Sn targets films are porous with open spaces and voids (Fig. 4a), but become denser whether when the bias voltage of Ag-doped Sn targets increases (Fig. 4b and c), or when the target–substrate distance is longer (Fig. 4b and d). The abrupt layer/substrate interfaces indicates a good adhesion of films on substrates. It is well known that, thanks to the high energy of sputtered atoms, adhesion of films deposited by sputtering is better than that obtained by other deposition methods, *e.g.* by thermal evaporation [15], and this can be seen as an advantage of sputtering deposition thin films from the application point of view. Film thickness, estimated from cross-section SEM images, ranges from ∼2 to ∼3 μm for films deposited at the target–substrate distance of 120 mm and reduces to ∼1 μm when the target–substrate distance increases to 200 mm (Table 1). It is worth to note that film thickness does not increase monotonically with the Ag-doped Sn targets bias voltage, whereas the sputtering yield of Ag-doped Sn targets, and thus the deposition rate, are increasing with their bias voltage. This can be explained by the fact that films deposited at higher bias voltages of Ag-doped Sn targets are denser as observed above. The increase of both lateral grain size and crystallite size, as well as the fact that films appear to be denser at high bias voltages of Ag-doped Sn targets, could be attributed to an enhancement of the surface mobility of deposited atoms due to a larger amount of energy from the arriving sputtered atoms that accommodated in the substrate. On the other hand, the considerably lower deposition rate at the longer target–substrate distance promotes the surface diffusion of adatoms during film growth, therefore films are more compact and exhibit bigger grain size and crystallite size. Again, the same behavior for crystallite size and cross-section morphology is observed regardless of the type of substrate Si (1 0 0), Si (1 1 1), or fused silica.

Owing to the high reactivity of the Mg, oxidation of thin films during growth and more importantly when exposed to air is of a great concern. The oxidation rate depends on the rather porous microstructure of the films so exhibiting pathways which enhance the diffusion of oxygen. Effectively, after a long period exposure to air (*i.e.* weeks) all films change from a metallic brilliant surface right after deposition to a somewhat darker color. It is shown that porous thin films with excess Mg, *i.e.* films deposited at low bias voltage of Ag-doped Sn targets, exhibit an oxygen content up to 20 at.% oxygen after over one year of exposure to air. Films found to better resist to oxidation, *i.e.* the stoichiometric and dense Mg_2Sn films, are verified containing less than 3 at.% oxygen after over one year of exposure to air. In addition no significant increase of resistivity with this type of films further confirms the above assumption.

3.2. Thermoelectric performance of thin films

Preliminary characterization of thermoelectric performance at room temperature for deposited Mg_2Sn thin films is shown in Table 2. All doped films show positive Seebeck coefficients, while those of undoped films are negative, in good agreement with those results already reported for bulk materials [20,21]. Observation of a positive Seebeck coefficient for doped films corroborates well with their positive Hall voltages as revealed by Hall effect measurements and thus validates the role of Ag impurity as *p*-dopant. Films deposited at low bias voltages of Ag-doped Sn target (*i.e.* at −100 V and −200 V) exhibit high electrical conductivities and low Seebeck coefficients, consistent with a Mg-rich composition as revealed by EDS and XRD analysis. The Sn-rich film, *i.e.* film deposited at the bias voltage of Ag-doped Sn targets of −300 V, shows much lower σ and significantly higher S. The electrical conductivity of doped films is substantially higher than that of undoped films, indicating the role of Ag impurity. The values of electrical conductivity and Seebeck coefficient for both doped and undoped stoichiometric Mg_2Sn films (*i.e.* films deposited with Ag-doped Sn targets or pure Sn targets biased at −250 V) are in good agreement with reported results for Ag-doped and undoped bulk polycrystalline Mg_2Sn [20,21]. In fact, for the target–substrate distance of 120 mm, film with stoichiometric Mg_2Sn shows the highest power factor, which is $\sim 4.35 \times 10^{-3}$ W K^{-2} m^{-1}. On the other hand, at same bias voltages of Ag-doped Sn targets, the electrical conductivity of deposited films increases significantly, while the Seebeck coefficient decreases, as the target–substrate distance increases from 120 to 200 mm. These results are in agreement with above observation that films deposited at the higher target–substrate distance are denser and exhibit bigger grain and crystallite size. For the target–substrate distance of 200 mm, thin film deposited with bias voltage of Ag-doped Sn targets of −250 V exhibits the electrical conductivity nearly two orders of magnitude greater than that of undoped single crystal Mg_2Sn [22]. Thin film deposited in this condition (−250 V, 200 mm) therefore exhibits the room temperature power factor reaching the value of $\sim 5.02 \times 10^{-3}$ W K^{-2} m^{-1}, *i.e.* comparable to that of Bi_2Te_3-based thermoelectric compounds. Considering the fact that deposited thin films have polycrystalline nature and exhibit nano-size crystallites we could expect a lower thermal conductivity than that of the same materials in single crystalline or polycrystalline bulk form, which is about 5–7 W m^{-1} K^{-1} [21]. The best figure of merit ZT at room temperature of the deposited thin films thus should be better than 0.3.

4. Conclusions

Well crystallized and fine-grained C15 polycrystalline Mg_2Sn thin films with stoichiometry and microstructure well controlled are deposited on both silicon and glass substrates at room temperature by co-sputtering of individual targets, assisted by multi-dipolar microwave plasma. The study on the influence of various deposition parameters, which can be tuned independently in this co-sputtering deposition technique, demonstrates that chemical composition, microstructure and crystal structure of deposited thin films can be controlled with a fair reproducibility. The C14 hexagonal phase of Mg_2Sn formed under non-equilibrium conditions is observed for certain deposition conditions. Preliminary characterizations of TE performance show that

stoichiometric Mg_2Sn thin films doped with ~1 at.% Ag exhibit a high power factor at room temperature, which can reach the value of $\sim 5.02 \times 10^{-3}\,W\,K^{-2}\,m^{-1}$. Influence of nanosize grains on the reduction of the thermal conductivity of deposited thin films should be further investigated. Results of this work have allowed us to continue with the deposition of thin films of the Mg_2Si-Mg_2Sn solid solutions, whose ZT_{max} = 1.1 at ~800 K was recently reported in bulk form.

Acknowledgements

Authors wish to thank Richard Haettel (Institut Néel) for help in the preparation of Ag-doped tin targets and Daniel Bourgault (Institut Néel) for help with Seebeck coefficient measurement. One of the authors (H. Le-Quoc) received scholarships from the French Ministry of Research and Higher Education and the Rhône-Alpes region.

References

[1] D.M. Rowe (Ed.), Thermoelectrics Handbook: Macro to Nano, CRC Press, New York, 2006.
[2] E.N. Nikitin, V.G. Bazanov, V.I. Tarasov, Sov. Phys. Solid State 3 (1961) 2648.
[3] V.K. Zaitsev, M.I. Fedorov, E.A. Gurieva, I.S. Eremin, P.P. Konstantinov, A.Yu. Samunin, M.V. Vedernikov, Phys. Rev. B 74 (2006) 045207.
[4] W. Luo, M. Yang, F. Chen, Q. Shen, H. Jiang, L. Zhang, Mater. Sci. Eng. B 157 (2009) 96.
[5] M.S. Dresselhaus, G. Chen, M.Y. Tang, R. Yang, H. Lee, D. Wang, Z. Ren, J.P. Fleurial, P. Gogna, Adv. Mater. 19 (2007) 1–12.
[6] R. Venkatasubramanian, E. Siivola, T. Colpitts, B. O'Quinn, Nature 413 (2001) 597–602.
[7] L. Chuang, N. Savvides, T.T. Tan, S. Li, J. Electron. Mater. 39 (2009) 1971–1974.
[8] K. Wasa, M. Kitabatake, H. Adachi, Thin Films Material Technology: Sputtering of Compound Materials, Springer, 2004.
[9] J. Pelletier, Distributed ECR plasma sources, in: O. Popov (Ed.), High Density Plasma Sources: Design, Physics and Performance, Noyes Publications, New Jersey, 1995, pp. 380–422.
[10] S. Béchu, O. Maulat, Y. Arnal, D. Vempaire, A. Lacoste, J. Pelletier, Surf. Coat. Technol. 186 (2004) 170.
[11] M.A.A.J. Lieberman, Litchtenberg in Principles of Plasma Discharges and Materials Processing, Wiley, 2005, p. 308.
[12] J. Rodriguez-Carvajal, Newsletter 26 (2001) 12.
[13] P. Thompson, D.E. Cox, J.B. Hastings, J. Appl. Cryst. 20 (1987) 79.
[14] B.D. Cullity, S.R. Stock, Elements of X-ray Diffraction, 3rd ed., Prentice-Hall Inc, 2001, pp. 167–171.
[15] L. Maissel, Application of sputtering to the deposition of films, in: L.I. Maissel, R. Glang, (Eds.), Handbook of Thin Film Technology, McGraw-Hill Publishers, 1970, pp. 4.10–4.13.
[16] T.I. Dyuzheva, S.S. Kabalkina, L.F. Vereshchagin, Sov. Phys. Crystallogr. 17 (1973) 705.
[17] G. Urretavizcaya, G.O. Meyer, J. Alloys Compd. 339 (2002) 211–215.
[18] D. Boudemagh, D. Fruchart, R. Haettel, E.K. Hlil, A. Lacoste, L. Ortega, N. Skryabina, J. Tobola, P. Wolfers, Solid State Phenomena 170 (2011) 253–258.
[19] J.A. Thornton, J. Vac. Sci. Technol. 11 (1974) 666–670.
[20] H.Y. Chen, N. Savvides, T. Dasgupta, C. Stiewe, etE. Mueller, Phys. Status Solid. A 207 (2010) 2523–2531.
[21] H.Y. Chen, N. Savvides, J. Cryst. Growth 312 (2010) 2328–2334.
[22] L.D. Crossmann, G.C. Danielson, Phys. Rev. 171 (1968) 867–875.